Formation of Deep-Subwavelength Structures on Organic Materials by Femtosecond Laser Ablation

Lei Wang, Xiao-Wen Cao, Chao Lv, Hong Xia, Wen-Jing Tian, Qi-Dai Chen, Saulius Juodkazis, and Hong-Bo Sun, *Member, IEEE*

***Abstract*— Femtosecond (fs-) laser induced subwavelength and deep-subwavelength periodic structures have attracted attention due to their sub-diffraction feature size and rich physics of laser-matter interaction. However, the formation mechanisms of fs-laser induced deep-subwavelength structures on organic materials have not been reported nor systematically studied. Herein, based on the degree of laser induced free-carrier excitation, the formation of deep-subwavelength structures by fs-laser ablation was systematically studied on popular materials: negative tone resists SU8 and conductive polymer poly-3, 4-ethylenedioxythiophene: poly-(styrenesulfonate) (PEDOT: PSS). A weak propensity to form deep-subwavelength structures was found on poly-methylmethacrylate and polyvinyl alcohol. The photo-excited electrons forming the surface plasmonic wave contributed to energy localization and absorption, which led to the imprinting of deep-subwavelength structures on polymers. It has been found that materials with π-bonds and benzene rings were most susceptible to deep-subwavelength structure formation. Based on a laser-induced surface plasmonic model, the period of regular patterns was estimated and was in a good accordance with experimental results. The proposed formation mechanism of the deep-subwavelength structures on organic materials extends an application field of fs-laser micro/nanomachining of polymers.**

***Index Terms*— Femtosecond laser induced periodic structures, deep-subwavelength structures, organic materials, plasmonic ablation**

I. Introduction

FEMTOSECOND (fs-) laser induced periodic structures (LIPSS) have attracted attention due to their sub-diffraction period and ability to nanostructure surfaces and inner volume of materials [1]. Also a rich physics of light-matter interaction reveals different material relaxations resulting in nanoscale modifications [2]–[8]. Two kinds of polarization dependent structures have been observed so far. One kind is termed near-subwavelength structures (NSWS) with a period close to the irradiation wavelength, caused by the interference of incident light and the scattered light [3], [5], [9], [10]. The other kind is termed deep-subwavelength structures (DSWS) with a period less than 1/3 wavelength, which is due to the laser-excited electrons and surface wave [2], [3], [10]–[13]. Up to now, it has become a generic fs-laser ablation phenomenon on the surface or in the bulk of nearly all inorganic materials, such as metals, [2], [14], [15] semiconductors, [2], [16]–[20] and insulators [2], [21]. However, only a few cases of structuring on organic materials have been reported, including popular polycarbonate (PC), polytrimethylene terephthalate (PTT) and poly-ethylene terephthalate (PET) [22]–[26], opto-electric materials poly-3-hexylthiophene (P3HT) [27], and biomaterials poly-L-lactic acid (PLLA) [28]. These studies have shown potential for applications in SERS [23], bio-science [25], [28], and optoelectric-devices [27]. Nevertheless, fs-laser induced DSWS on organic materials have not been studied nor systematic attempts were made to create nanoscale structures different from the Rayleigh-Taylor instabilities (RTI) in molten phase [29]. The period of RTI patterns is given by $P = (\sigma h/\rho)^{1/4}(2\pi\tau_l)^{1/2}$, where σ is the surface tension of molten material, h is its height, ρ is its density, τ_l is the lifetime of the molten phase before solidification.

Herein, we report a study of fs-laser induced DSWS on the surface of a series of materials qualitatively classified by the degree of electronic excitation, which include: (i) easy to be optically excited such as SU8 photoresist with a narrower effective bandgap; (ii) having comparable free carriers with metals, poly-3,4-ethylenedioxythiophene: poly-(styrenesulfonate) (PEDOT: PSS); and (iii) hard to be excited (wide bandgap) as polymethylmethacrylate (PMMA) and polyvinyl alcohol (PVA). Uniform periodic DSWS were obtained on SU8 and PEDOT: PSS while only some signs of DSWS were found on PMMA and PVA at the ablation pits. Electrons excited by bond breaking and contributing to the surface plasma wave were analyzed in terms of chemical specificity, namely, the π-bond of C = C and delocalized π-bond of benzene ring correlated with propensity of sub-

Manuscript received May 27, 2017; revised August 7, 2017 and September 10, 2017; accepted September 12, 2017. Date of publication September 15, 2017; date of current version January 22, 2018. This work was supported in part by the National Key Research and Development Program of China and National Natural Science Foundation of China under Grant 2017YFB1104600, Grant 61590930, Grant 2014CB921302, Grant 61435005, and Grant 51335008, and in part by the Changjiang Scholar Program of Chinese Ministry of Education. *(Corresponding author: Qi-Dai Chen.)*

L. Wang, X.-W. Cao, C. Lv, H. Xia, Q.-D. Chen, and H.-B. Sun are with the State Key Laboratory of Integrated Optoelectronics, College of Electronic Science and Engineering, Jilin University, Changchun 130012, China (e-mail: chenqd@jlu.edu.cn).

W.-J. Tian is with the State Key Laboratory of Supramolecular Structure and Materials, College of Chemistry, Jilin University, Changchun 130012, China.

S. Juodkazis is with the Centre for Micro-Photonics, Faculty of Science, Engineering and Technology, Swinburne University of Technology, Hawthorn, VIC 3122, Australia, and also with the Melbourne Centre for Nanofabrication, ANFF, Clayton, VIC 3168, Australia.

Color versions of one or more of the figures in this paper are available online at http://ieeexplore.ieee.org.

Digital Object Identifier 10.1109/JQE.2017.2753040

wavelength structure formation. Based on the laser-induced plasma model, the period was estimated and found to be in a good agreement with the experiment results. We have chosen fs-laser pulses to explore the DSWS formation on polymers to reduce effects of laser induced melting and hydrodynamic instabilities which are known to cause nanoscale features including periodic patterns upon solidification as in the case of RTI.

II. Experiments and Materials

All the films with thickness of about 500 nm were made on a cleaned glass by spinning. The SU8 2025 photoresist (MicroChem Corp.) diluted by cyclopentanone at a ratio 1:9 and PEDOT: PSS solution (Xi'an Polymer Light Technology Corp.) was deposited at spinning speed of 3000 rpm, respectively. While the PMMA (Aladdin Industrial Corp.,) in chloroform (wt5%) and PVA (Aladdin Industrial Corp.,) aqueous solution (wt5%) were deposited at spinning speed of 5000 rpm, respectively. Near infrared fs-laser pulses were delivered by a Ti:sapphire regenerative amplifier laser system (Spectra Physics) operating at the 800 nm wavelength. The pulse duration was 100 fs and the repetition rate was 1 kHz. Laser beam was expanded from 8 mm to 16 mm in diameter and reshaped by a rectangular mask with a hole of 8 mm long and 2 mm wide. A cylindrical lens with a focal length f = 35 mm was used to focus the beam into a uniform linear shape of $L = 8$ mm in length and about $W = 8$ μm in width. Scanning with different velocities was conducted perpendicular to the cylindrical long-axis of the focal spot to observe the evolution of DSWS. The laser power of P was measured after the mask while the laser fluence F was estimated by $F = P/(W \times L \times 1000\ \text{Hz})$. The "quill" effect – a different morphology upon reciprocating directions of linear scan - on SU8 was observed by writing with an objective lens (10×, numerical aperture $NA = 0.25$).

III. Femtosecond Laser Induced DSWS on Organics Materials

SU8 is a popular negative photoresist which is widely used for fs-laser three-dimensional (3D) printing of functional structures and devices through a photo-initiated crosslinking process [30], [31]. Although SU8 is not conductive, electrons could still be excited below the ablation threshold by opening the epoxy group and amplified via an acid catalysis [31]–[33]. DSWS were observed on the SU8 film without crosslinking (Fig. 1). The period evolution was explored by using a cylindrical lens focusing and scanning, which has advantages in a large-area uniform structure fabrication [34]. The formed periodic structures become more obvious as the scanning speed decreased, which was attributed to the similar pulse accumulation effect as in the inorganic materials [17]. When the scanning speed was 20 μm/s ($W/(20\mu\text{m/s}) \times 1\ \text{kHz} = 400$ pulses per spot), only a few traces of DSWS appeared around some of the ablation pits (Fig. 1a). The traces became more obvious and connected to each other at a slower speed of 10 μm/s (800 pulses per spot; Fig. 1b). The most uniform structures were obtained when the speed was down to 6 μm/s (1333 pulses per spot; Fig. 1c). However,

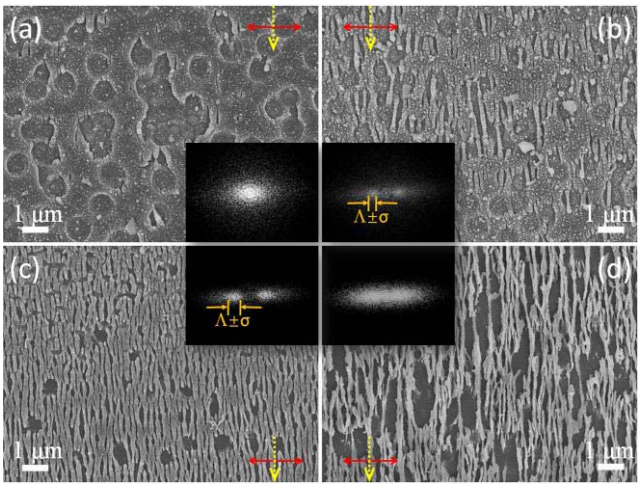

Fig. 1. DSWS formation on SU8 film irradiated at different scanning speeds: (a) 20 μm/s, (b) 10 μm/s, (c) 6 μm/s, and (d) 2 μm/s. FFT results show the period $\Lambda \pm \sigma$ is 240 ± 70 nm. The red arrow and the yellow dashed arrow represent the polarization and scanning directions, respectively. Scale bars for (a-d) are 1 μm.

if the speed was too slow, 2 μm/s (about 4000 pulses per spot), some regions in the DSWS area had caused a strong ablation (Fig. 1d). The fast Fourier transform (FFT) analysis of SEM images by software Image J, which is making the convolution of the grey levels, revealed the period value and orientation. The period $\Lambda \pm \sigma$ of the structures, 240 ± 70 nm, was obtained, where Λ was the average value and σ was the mean square deviation. All the structures were found aligned vertically to the laser polarization, which is the same as those reported for the inorganic materials (also known as the normal DSWS with anomalous-DSWS being rotated by 90-degrees). Threshold for the laser ablation of SU8 was about 100 mJ/cm^2 while the laser irradiance used for DSWS printing was 375 mJ/cm^2. The scanning direction was perpendicular to the laser polarization.

The similarity of the LIPPS on these polymers to the structures reported on inorganic substrates invites to explore the formation of DSWS via the laser-induced electronic excitation. A phenomenon of structure period splitting was observed on SU8 at speed of 10 μm/s with period only about 105 nm, as well as some secondary nano-gratings with period of several tens nanometers; this was similar to the patterns reported on gallium nitride [35] (Fig. 2a). The width of irradiation traces was increasing along the scan direction (Fig. 2b), reminiscent to the "quill" writing effect in inorganic materials due to the pulse front tilt [36]–[38]. These similarities in morphology of DSWS in inorganic materials [3], [4], [17] indicates that similarities in electronic excitation and laser-induced chemical bond breaking exist.

From the Fourier-transform IR (FTIR; NICOLET 6700) absorbance data, the changes in both epoxy group (at 862 cm^{-1}, 914 cm^{-1}, and 972 cm^{-1}) and C-H bond of the benzene ring (at 972 cm^{-1}) represents a process of an electron transfer [33] (Fig. 2c). The benzene skeleton was kept stable before and after laser irradiation as evidenced at the features at the wavenumbers 1608 cm^{-1}, 1582 cm^{-1}, and

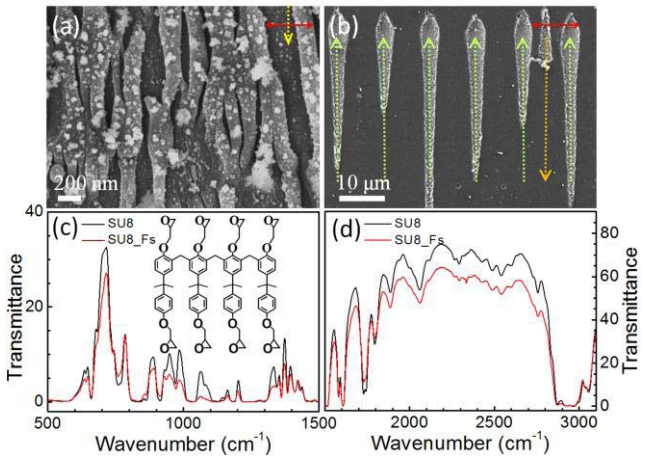

Fig. 2. Structure formation and electronic excitation revealed by FTIR. (a) Typical structures and feature sizes. (b) Width was increasing along the scan direction due to the laser driven charge transfer and heating. (c-d) FTIR results of SU8 before (the black dash line) and after laser modification (the red dash line named SU8_Fs). The red arrow and the yellow dashed arrow represent the polarization and scanning directions, respectively. Scale bars are 200 nm in (a) and 10 μm in (b), respectively.

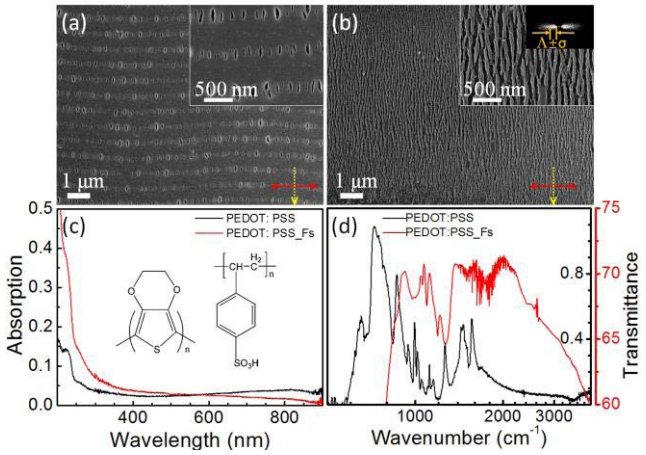

Fig. 3. DSWS on PEDOT: PSS. (a) DSWS formed by scanning at 50 pulses per focal spot. (b) DSWS by scanning 500 per spot. (c) UV before (the black dashed line) and after laser scanning (the red dashed line). (d) FTIR spectra before and after laser scanning. The red arrow and the yellow dashed arrow represents the polarization and scanning directions, respectively. Scale bars are 1 μm and 500 nm for the panel and inset figures, respectively.

1505 cm^{-1}. The C-O bond at 1184 cm^{-1} and 1296 cm^{-1} was unchanged before and after the laser ablation. Furthermore, large changes of peak shape from 900 cm^{-1} to 1300 cm^{-1} represent the laser induced process which affected the C-S bond on the three-phenyl-sulfide and micro/nanostructure formation on the surface of SU8. Hence, it can be deducted that the excited electrons mainly come from laser induced breakdown of the epoxy group, C-H bond on the benzene ring and, to a lesser extent, from C-S bond. Crosslinking was not affecting the DSWS formation and similar structures were obtained on the crosslinked SU8 film.

Understandably, the DSWS were easily demonstrated on PEDOT: PSS, which is widely used for electrodes for organic light-emitting diode (OLED) due to its electrical conductivity comparable with that of metals [39] (Fig. 3a-b). At 50 pulses

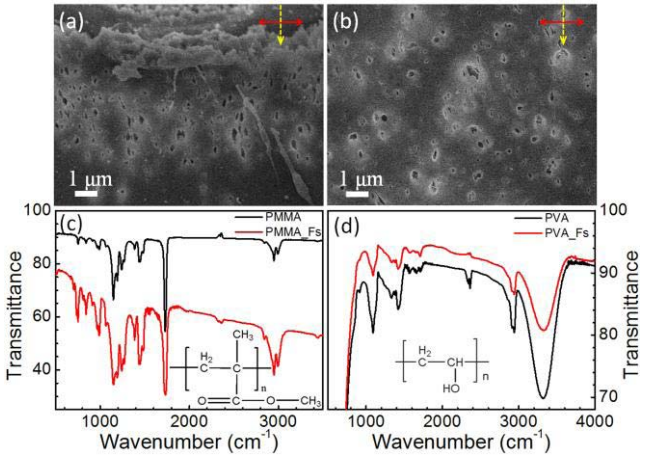

Fig. 4. DSWS on PMMA and PVA. (a-b) Laser induced patterns on PMMA and PVA, respectively. (c-d) FTIR spectra of PMMA and PVA before (the black dash lines) and after laser scanning (the red dash lines). The red arrow and the yellow dashed arrow represent the polarization and scanning directions, respectively. Scale bars are 1 μm.

per focal spot diameter for every focal scan using cylindrical lens, periodical nanocracks perpendicular to the laser polarization were found breaking the film with a period 280 $\pm$ 60 nm (Fig. 3a). When the scanning speed was 16 μm/s, (about 500 pulses per spot), the cracks became connected to each other to form large-area periodic nanogratings. Period $\Lambda \pm \sigma$ become 120 $\pm$ 60 nm as shown in the inset FFT image in Fig. 3b. Laser fluence was about 200 mJ/cm^2, and scanning direction was perpendicular to the polarization. After laser modification, the film acquired a black tint in a visible region (Shimadzu UV-3600 spectrometer) which can be attributed to the surface texturing (Fig. 3c). However, it becomes much more transparent in the infrared waveband in the FTIR spectra, due to the bond break. Shown in Fig. 3d, all the bonds including C-C, C = C, C-S, C-O, C-H, and the number density of benzene ring have dramatically decreased due to the strong ionization induced by laser irradiation. Threshold for the laser ablation of PEDOT:PSS was about 78 mJ/cm^2 while the laser irradiance used for DSWS printing was 313 mJ/cm^2. The scanning direction was perpendicular to the laser polarization.

Interestingly, it was not possible to imprint uniform periodic DSWS patterns on some of the organic materials. PMMA is polymerized by methylmethacrylate (MMA) made of C-C, C-O, C = O, and C-H bonds which are among the strongest and cannot be easily photo-excited. Only some hints of structures were observed with irregular period 187 $\pm$ 20 nm (Fig. 4a). FTIR results show a uniform decrease of peaks in transmittance which could be attributed to the carbonization under high laser irradiation fluence. Similarly, signs of DSWS and decreased transmittance were also observed in laser damaged PVA with irregular period 184 $\pm$ 27 nm. Irradiance used for PMMA structuring was 100 mJ/cm^2 and 300 mJ/cm^2 for PVA while the thresholds were 80 mJ/cm^2 and 50 mJ/cm^2, respectively. Scanning direction was perpendicular to the polarization with scanning speed 10 μm/s (800 pulses per spot).

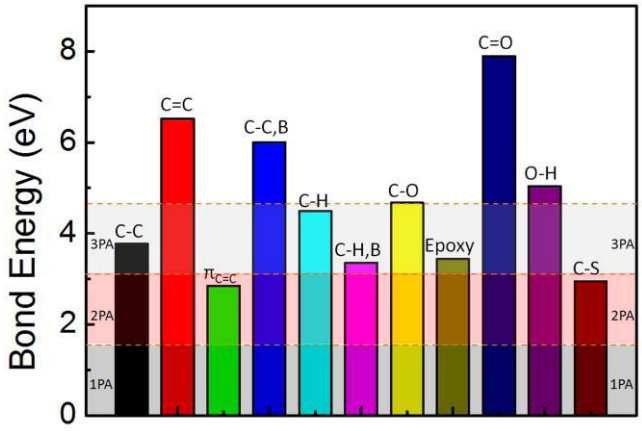

Fig. 5. Chemical bond energy for the different bonds and comparison with the laser photon energy and one, two, three-photon absorption.

By comparison of the bond strength (energy) [40] with laser photon energy (1.55 eV for 800 nm wavelength or 1 eV = 96.4 kJ/mol), the reasons for the formation of periodic DSWS could be qualitative understood via electronic excitation (a chemical bond breaking) similarly to the inorganic materials [41] (Fig. 5). Multi-photon absorption is required to liberate the bonding electrons. The π-bond of C = C and the C-S bond have the lowest energy which need only two-photon absorption (2PA) at the wavelength of 800 nm to excite electrons of the bonds. The C-C, C-H, and C-H bond of benzene ring, C-O, and epoxy group bond required 3-photon absorption (3PA) for excitation of electrons. The strongest O-H, C-C bond of the benzene ring and C = O have even a larger required energy to excite electrons via the multi-photon absorption. But, according to the power scaling of absorption, for the higher order nonlinear processes [42], a larger intensity is required and, obviously, a stronger ablation occurred with increasing intensity.

It is worth noting that the C-C bond in aliphatic compounds and C-C bond of benzene ring in aromatic compounds are defining the threshold of ablation in organic material. Electronic excitation should be below the energy of C-C bond or C-C bond of benzene ring in order to have ablation by the lowest order multi-photon process, the 2PA. Because energy of C = C with the π-bond is smaller than that of C-C bond, a laser processing of materials with the C = C bonds is much easier. Contrarily, it is less probable to obtain uniform periodic DSWS pattern in materials without π-bonds such as PMMA and PVA. Energy of C-C in benzene ring is between of that in C-C and C = C, which provides a larger energy window for possible laser structuring as observed in SU8 photoresist.

The qualitative picture of dielectric breakdown discussed above is consistent with fs-laser writing which occurs at the lower irradiance via the controlled avalanche ionization [43]. At the irradiance/intensity larger than the ablation threshold, a contribution via nonlinear multi-photon absorption is increasing faster as compared with the avalanche absorption which is dominant at the laser polymerization in direct laser 3D printing [43]. Both nonlinear mechanisms are important for the surface ablation and nanostructure pattern formation.

IV. Plasmonic Ablation Model

The free carriers generated by absorption (bond breaking) were responding collectively to incident light by oscillating in resonance with the fs-laser electric field, i.e., defining the surface plasmonic excitation [13, 44, 45] which was changing the permittivity [46]. Based on the plasmonic model [3, 17], the Drude equation was used to describe the permittivity of the laser-excited layer which supports the plasmonic standing wave for deep-subwavelength structure formation. The effective dielectric constant of the active layer $\varepsilon*$ changed as the laser excited carrier concentration n_{eh} [2],[17],[47]:

$$\varepsilon* = 1 + (\varepsilon_{\rm n}-1)(1-\frac{n_{eh}}{n_0}) - \frac{w_p^2}{w^2}\frac{1}{1+i(w\tau_D)^{-1}}, \quad (1)$$

$$\text{where,} \quad {\rm w} = \frac{2\pi {\rm c}}{\lambda}, \quad w_p^2 = \frac{n_{eh}e^2}{\varepsilon_0 m_{opt} m_e}, \quad (2)$$

λ is the laser wavelength 800 nm, m_{opt} is the effective electron mass, m_e is the electron mass, ε_0 is the vacuum permittivity, e is the single electron charge, c is the light speed in vacuum, $\rm n_0$ is the valance electron density, ε_n is the material dielectric constant at the wavelength of 800 nm, w_p is the plasma frequency, and τ_D is the electron damping time.

Considering the environment is air, $\varepsilon_d = 1$, the effective dielectric constant ε wasshown as given [17]:

$$\frac{1}{\varepsilon} = \frac{1}{\varepsilon*} + \frac{1}{\varepsilon_s}, \quad n = \sqrt{\varepsilon}, \quad (3)$$

where $\varepsilon_{\rm s}$ represents the effective dielectric constant of the external environment defined by the volume fraction of air and substrate. Because the surface plasmon would transport along the interface between the air and organic deep-subwavelength structure surface [47], the volume fraction of material x was defining the effective dielectric function of the deep-subwavelength structure:

$$\varepsilon_{\rm s} = x\varepsilon_{\rm n} + (1-x)\varepsilon_{\rm d}. \quad (4)$$

The surface plasmonic wavelength λ_{sp} was defined by the [17]:

$$\lambda_{\rm sp} = \frac{2\pi}{k_{sp}}, \quad \text{while } K_{sp} = \frac{\rm w}{c/{\rm n}} = k_{sp} + i\,I_{sp}, \quad (5)$$

where K_{sp}, k_{sp}, and I_{sp} are the complex, real part, and imaginary part of wavevector, respectively. The period of DSWS, Λ_{DSWS}, is defined as the half of the λ_{sp} by the condition of the standing plasmon wave existing on the plasma surface, for which the wavevector matching can be satisfied at the smallest period. This standing wave was finally imprinted on the surface by ablation:

$$\Lambda_{DSWS} = \lambda_{sp}/2. \quad (6)$$

Parameter values were estimated and summarized in Table 1. Density of the valance electrons was calculated by:

$$\rm n_0 = k_0 \rho N_a / M, \quad (7)$$

where N_a is the Avogadro constant and M is the monomer molar mass. For the stable chemical compound, the density of valence electrons is calculated by their valence state according to the monomer molecular formula, k_0 is the total valence

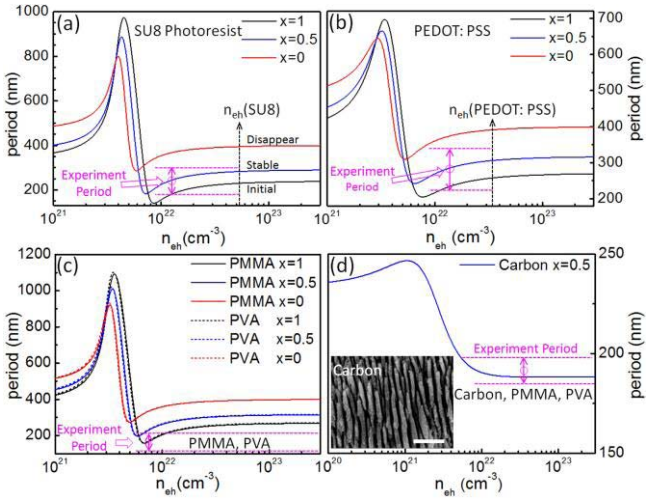

Fig. 6. Period calculation by surface plasma wave model. (a-d) Simulated periods on photoresist of SU8, conductive polymer of PEDOT: PSS, PMMA, PVA, and carbon. The inset figure in (d) shows the DSWS on carbon with scale bar of 1 μm.

TABLE I

PARAMETERS USED IN CALCULATION FOR DEEP-SUBWAVELENGTH STRUCTURES

Mater	Formula	n	k	ρ g/cm^3	M g/mol	k_0	n_0 10^{23}/cm^{-3}	m_{opt}	τ_D (fs)
SU8[49]	$C_{22}O_4H_{24}$	1.67	0.001	1.18	338	120	2.52	0.8	3
PEDOT[50]	$C_6O_2H_4S$	1.48	0.1	1.01	140	34	1.48	0.1	1
PMMA[51]	$C_5O_2H_8$	1.49	0.001	1.17	100	32	2.82	0.8	3
PVA[52, 53]	C_2OH_4	1.47	0.001	1.27	44	14	4.2	0.8	3
Carbon[54]	C	2.40	1.55	2.25	12	4	4.5	0.1	3

number of electrons in monomer. For example, k_0 equals to $4 \times 22 + 2 \times 4 + 1 \times 22 = 120$ in each molecular of SU8 with formula $C_{22}O_4H_{24}$. Because m_{opt} and τ_D took little effect on the final stable period value, they are set to 0.8 and 3 fs for SU8, PMMA, and PVA, and 0.1, 1 fs for PEDOT. Such values are typical for inorganic glass [48].

Taking SU8 as an example, the plasmonic wavelength (Fig. 6(a)) calculated by Eq. (4) reaches saturated values for the carrier densities larger than 9×10^{22} cm^{-3}. Considering the free electrons are generated by bond breaking (shown in Fig 5), the maximum number density could approach that of valance electrons and is produced out of four epoxy group bonds and two C-H bonds on the benzene ring, which contributes $4 \times 2 + 2 \times 8 = 24$ electrons with electron density n_{eh}(SU8) $= 5.04 \times 10^{22}$ cm^{-3}. This is enough to obtain a stable period for deep-subwavelength structures.

Once the surface grating is formed, the x value is changing causing the evolution of deep-subwavelength structures. The case of x = 1 (a flat surface) was the initial condition of the plasmonic imprinting and defined the lower bound for the period observed in experiments. For the case x = 0, the upper bound limit of the period was obtained. The air-substrate ratio in experiments was usually around 0.5, which corresponds to the experimental period of 240 ± 70 nm. Period observed on PEDOT: PSS showed a similar trend as SU8 and is in good agreement with the model (Fig. 6 (b)). The excited electron density n_{eh}(PEDOT: PSS) was 3.47×10^{22} cm^{-3} (two π-bonds of C = C and two C-S bonds, $2 \times 2 + 2 \times 2 = 8$ electrons in each molecule). Due to the carbonization, the period on PMMA and PVA was far below the simulation predictions but around the estimated period of carbon at x = 0.5 (Fig 6(c-d)).

Organic materials are rapidly emerging as superior replacements for a number of applications. The sub-diffraction laser-induced periodic structures have unique properties for applications in surface nano-texturing, e.g., surface energy modification for superhydrophobicity and self-cleaning, surface refractive index modification for antireflection, and surface area increase required for sensors and nano-electronics.

V. CONCLUSIONS

Uniform periodic deep-subwavelength structures on organic materials have been demonstrated on negative photoresist SU8 with periods of 240 ± 70 nm (∼1/3 λ) and PEDOT: PSS with period 280 ± 60 nm (∼1/3 λ), 120 ± 60 nm (∼1/7 λ), respectively. While only weak sign of deep-subwavelength structure was observed on PMMA and PVA, ∼190 nm (∼1/4λ). Similar to inorganic materials, scanning speed affected the structure periodicity and uniformity. The structure splitting and "quill"- accumulation effect affected the excitation of electrons and the formation of the plasmonic layer which were important in the final structure formation. Based on FTIR data before and after laser modification, it can be concluded that materials with π-bonds and more stable benzene rings can be patterned by deep-subwavelength structures easier due to the propensity to electronic excitation. Laser-induced surface plasmonic model was applied to estimate the period and showed a good agreement with experiment results. The proposed high spatial frequency laser induced periodic structures on organic materials expands a nanoscale fabrication capability of fs-laser micro/nanomachining onto surfaces of polymers.

REFERENCES

[1] B. Öktem *et al.*, "Nonlinear laser lithography for indefinitely large-area nanostructuring with femtosecond pulses," *Nature Photon.*, vol. 7, pp. 897–901, Nov. 2013.
[2] J. Bonse, S. Höhm, S. V. Kirner, A. Rosenfeld, and J. Krüger, "Laser-induced periodic surface structures—A scientific evergreen," *IEEE J. Sel. Topics Quantum Electron.*, vol. 23, no. 3, May 2017, Art. no. 9000615.
[3] R. Buividas, M. Mikutis, and S. Juodkazis, "Surface and bulk structuring of materials by ripples with long and short laser pulses: Recent advances," *Prog. Quantum Electron.*, vol. 38, pp. 119–156, May 2014.
[4] K. Sugioka and Y. Cheng, "Ultrafast lasers–reliable tools for advanced materials processing," *Light Sci. Appl.*, vol. 3, p. e149, Apr. 2014.
[5] J. Bonse, A. Rosenfeld, and J. Krüeger, "On the role of surface plasmon polaritons in the formation of laser-induced periodic surface structures upon irradiation of silicon by femtosecond-laser pulses," *J. Appl. Phys.*, vol. 106, p. 104910, Nov. 2009.
[6] F. Garrelie *et al.*, "Evidence of surface plasmon resonance in ultrafast laser-induced ripples," *Opt. Exp.*, vol. 19, pp. 9035–9043, May 2011.
[7] M. Malinauskas *et al.*, "Ultrafast laser processing of materials: From science to industry," *Light Sci Appl.*, vol. 5, p. e16133, Aug. 2016.
[8] Y. Matushiro, S. Juodkazis, K. Hatanaka, and W. Watanabe, "Regenerated volume gratings in PMMA after femtosecond laser writing," *Opt. Lett.*, vol. 42, p. 1632, Apr. 2017.

[9] M. Huang, F. Zhao, Y. Cheng, N. Xu, and Z. Xu, "Origin of laser-induced near-subwavelength ripples: Interference between surface plasmons and incident laser," *ACS Nano*, vol. 3, pp. 4062–4070, Dec. 2009.

[10] Y. Pan *et al.*, "Threshold dependence of deep- and near-subwavelength ripples formation on natural MoS_2 induced by femtosecond laser," *Sci. Rep.*, vol. 6, p. 19571, Jan. 2016.

[11] V. Khuat, J. Si, T. Chen, and X. Hou, "Deep-subwavelength nanohole arrays embedded in nanoripples fabricated by femtosecond laser irradiation," *Opt. Lett.*, vol. 40, pp. 209–212, Jan. 2015.

[12] M. Huang, F. Zhao, Y. Cheng, N. Xu, and Z. Xu, "Mechanisms of ultrafast laser-induced deep-subwavelength gratings on graphite and diamond," *Phys. Rev. B, Condens. Matter*, vol. 79, p. 125436, Mar. 2009.

[13] S. K. Das, H. Messaoudi, A. Debroy, E. McGlynn, and R. Grunwald, "Multiphoton excitation of surface plasmon-polaritons and scaling of nanoripple formation in large bandgap materials," *Opt. Mater. Exp.*, vol. 3, pp. 1705–1715, Oct. 2013.

[14] L. Gemini *et al.*, "Periodic surface structures on titanium self-organized upon double femtosecond pulse exposures," *Appl. Surf. Sci.*, vol. 336, pp. 349–353, May 2015.

[15] Y. Miyasaka, M. Hashida, T. Nishii, S. Inoue, and S. Sakabe, "Derivation of effective penetration depth of femtosecond laser pulses in metal from ablation rate dependence on laser fluence, incidence angle, and polarization," *Appl. Phys. Lett.*, vol. 106, p. 013101, Jan. 2015.

[16] M. Straub, M. Afshar, D. Feili, H. Seidel, and K. König, "Periodic nanostructures on Si(100) surfaces generated by high-repetition rate sub-15 fs pulsed near-infrared laser light," *Opt. Lett.*, vol. 37, pp. 190–192, Jan. 2012.

[17] L. Wang *et al.*, "Rapid production of large-area deep sub-wavelength hybrid structures by femtosecond laser light-field tailoring," *Appl. Phys. Lett.*, vol. 104, p. 031904, Jan. 2014.

[18] S. Höhm, A. Rosenfeld, J. Krüger, and J. Bonse, "Femtosecond diffraction dynamics of laser-induced periodic surface structures on fused silica," *Appl. Phys. Lett.*, vol. 102, p. 054102, Feb. 2013.

[19] P. Liu, L. Jiang, J. Hu, S. Zhang, and Y. Lu, "Self-organizing microstructures orientation control in femtosecond laser patterning on silicon surface," *Opt. Exp.*, vol. 22, pp. 16669–16675, Jun. 2014.

[20] C. Wang, H. Huo, M. Johnson, M. Shen, and E. Mazur, "The thresholds of surface nano-/micro-morphology modifications with femtosecond laser pulse irradiations," *Nanotechnology*, vol. 21, p. 075304, Jan. 2010.

[21] R. Buividas, S. Rekštytė, M. Malinauskas, and S. Juodkazis, "Nanogroove and 3D fabrication by controlled avalanche using femtosecond laser pulses," *Opt. Mater. Exp.*, vol. 3, no. 10, pp. 1674–1686, 2013.

[22] E. Rebollar, J. R. V. D. Aldana, J. A. Pérez-Hernández, T. A. Ezquerra, P. Moreno, and M. Castillejo, "Ultraviolet and infrared femtosecond laser induced periodic surface structures on thin polymer films," *Appl. Phys. Lett.*, vol. 100, p. 041106, Jan. 2012.

[23] E. Rebollar *et al.*, "Assessment of femtosecond laser induced periodic surface structures on polymer films," *Phys. Chem. Chem. Phys.*, vol. 15, pp. 11287–11298, May 2013.

[24] E. Rebollar *et al.*, "Physicochemical modifications accompanying UV laser induced surface structures on poly(ethylene terephthalate) and their effect on adhesion of mesenchymal cells," *Phys. Chem. Chem. Phys.*, vol. 16, pp. 17551–17559, Jul. 2014.

[25] Y. Sato, M. Tsukamoto, T. Shinonaga, and T. Kawa, "Femtosecond laser-induced periodic nanostructure creation on PET surface for controlling of cell spreading," *Appl. Phys. A, Solids Surf.*, vol. 122, p. 184, Feb. 2016.

[26] E. Rebollar, M. Castillejo, and T. A. Ezquerra, "Laser induced periodic surface structures on polymer films: From fundamentals to applications," *Eur. Polym. J.*, vol. 73, pp. 162–174, Dec. 2015.

[27] Á, Rodríguez-Rodríguez *et al.*, "Laser-induced periodic surface structures on conjugated polymers: Poly(3-hexylthiophene)," *Macromolecules*, vol. 48, pp. 4024–4031, Jan. 2015.

[28] S. Yada and M. Terakawa, "Femtosecond laser induced periodic surface structure on poly-L-lactic acid," *Opt. Exp.*, vol. 23, pp. 5694–5703, Mar. 2015.

[29] M. S. Trtica, B. M. Gakovic, B. B. Radak, D. Batani, T. Desai, and M. Bussoli, "Periodic surface structures on crystalline silicon created by 532 nm picosecond Nd: YAG laser pulses," *Appl. Surf. Sci.*, vol. 254, pp. 1377–1381, Aug. 2007.

[30] A. del Campo and C. Greiner, "SU-8: A photoresist for high-aspect-ratio and 3D submicron lithography," *J. Micromech. Microeng.*, vol. 17, pp. R81–R95, Jun. 2007.

[31] D. Wu *et al.*, "A facile approach for artificial biomimetic surfaces with both superhydrophobicity and iridescence," *Soft Matter*, vol. 6, pp. 263–267, Jan. 2010.

[32] H. A. De, B. Hommersom, and A. F. Koenderink, "Wavelength-selective addressing of visible and near-infrared plasmon resonances for SU8 nanolithography," *Opt. Exp.*, vol. 19, pp. 11405–11414, May 2011.

[33] D. Y. Kang, C. Kim, G. Park, and J. H. Moon, "Liquid immersion thermal crosslinking of 3D polymer nanopatterns for direct carbonisation with high structural integrity," *Sci. Rep.*, vol. 5, p. 18185, Dec. 2015.

[34] S. K. Das, K. Dasari, A. Rosenfeld, and R. Grunwald, "Extended-area nanostructuring of TiO_2 with femtosecond laser pulses at 400 nm using a line focus," *Nanotechnology*, vol. 21, p. 155302, Mar. 2010.

[35] K. Miyazaki and G. Miyaji, "Nanograting formation through surface plasmon fields induced by femtosecond laser pulses," *J. Appl. Phys.*, vol. 114, p. 153108, Oct. 2013.

[36] W. Yang, P. G. Kazansky, and Y. P. Svirko, "Non-reciprocal ultrafast laser writing," *Nature Photon.*, vol. 2, pp. 99–104, Jan. 2008.

[37] C. Hnatovsky *et al.*, "Fabrication of microchannels in glass using focused femtosecond laser radiation and selective chemical etching," *Appl. Phys. A, Solids Surf.*, vol. 84, pp. 47–61, Apr. 2006.

[38] P. G. Kazansky, W. Yang, and E. Bricchi, "Quill' writing with ultrashort light pulses in transparent materials," *Appl. Phys. Lett.*, vol. 90, p. 151120, Apr. 2007.

[39] M. Xu, J. Feng, Y.-S. Liu, Y. Jin, H.-Y. Wang, and H.-B. Sun, "Effective and tunable light trapping in bulk heterojunction organic solar cells by employing Au-Ag alloy nanoparticles," *Appl. Phys. Lett.*, vol. 105, p. 153303, Oct. 2014.

[40] S. J. Blanksby and G. B. Ellison, "Bond dissociation energies of organic molecules," *Accounts Chem. Res.*, vol. 36, pp. 63–255, Aug. 2003.

[41] D. S. Correa, M. R. Cardoso, V. Tribuzi, L. Misoguti, and C. R. Mendonca, "Femtosecond laser in polymeric materials: Microfabrication of doped structures and micromachining," *IEEE J. Sel. Topics Quantum Electron.*, vol. 18, no. 1, pp. 176–186, Jan. 2012.

[42] D. S. Corrêa, L. De Boni, L. Misoguti, I. Cohanoschi, F. E. Hernandez, and C. R. Mendonça, "Z-scan theoretical analysis for three-, four- and five-photon absorption," *Opt. Commu.*, vol. 277, pp. 440–445, Sep. 2007.

[43] M. Malinauskas, A. Žukauskas, G. Bičkauskaite, R. Gadonas, and S. Juodkazis, "Mechanisms of three-dimensional structuring of photopolymers by tightly focussed femtosecond laser pulses," *Opt. Exp.*, vol. 18, p. 10209, Apr. 2010.

[44] W. L. Barnes, A. Dereux, and T. W. Ebbesen, "Surface plasmon subwavelength optics," *Nature*, vol. 424, no. 6950, pp. 824–830, 2003.

[45] J. Noack and A. Vogel, "Laser-induced plasma formation in water at nanosecond to femtosecond time scales: Calculation of thresholds, absorption coefficients, and energy density," *IEEE J. Quantum Electron.*, vol. 35, no. 8, pp. 1156–1167, Aug. 1999.

[46] K. Sokolowski-Tinten and D. von der Linde, "Generation of dense electron-hole plasmas in silicon," *Phys. Rev. B, Condens. Matter*, vol. 61, pp. 2643–2650, Jan. 2000.

[47] L. Wang *et al.*, "Competition between subwavelength and deep-subwavelength structures ablated by ultrashort laser pulses," *Optica*, vol. 4, pp. 637–642, Jun. 2017.

[48] Y. Hayasaki, K. Iwata, S. Hasegawa, A. Takita, and S. Juodkazis, "Time-resolved axial-view of the dielectric breakdown under tight focusing in glass," *Opt. Mater. Exp.*, vol. 1, pp. 1399–1408, Dec. 2011.

[49] I. Roch, P. Bidaud, D. Collard, and L. Buchaillot, "Fabrication and characterization of an SU-8 gripper actuated by a shape memory alloy thin film," *J. Micromech. Microeng.*, vol. 13, no. 2, pp. 330–336, 2003.

[50] K. Ranganathan, D. Wamwangi, and N. J. Coville, "Plasmonic Ag nanoparticle interlayers for organic photovoltaic cells: An investigation of dielectric properties and light trapping," *Solar Energy*, vol. 118, pp. 256–266, Aug. 2015.

[51] N. Sultanova, S. Kasarova, and I. Nikolov, "Dispersion properties of optical polymers," *Acta Phys. Polonica A*, vol. 116, pp. 585–587, Oct. 2009.

[52] M. J. Schnepf *et al.*, "Nanorattles with tailored electric field enhancement," *Nanoscale*, vol. 9, pp. 9376–9385, Jun. 2017.

[53] A. G. Hadi *et al.*, "Study the effect of barium sulphate on optical properties of polyvinyl alcohol (PVA)," *Univ. J. Mater. Sci.*, vol. 1, pp. 52–55, Jan. 2013.

[54] (2016). [Online]. Available: https://refractiveindex.info/?shelf=main&book=C&page=Phillip

Lei Wang received the Ph.D. degree in microelectronics from the College of Electronic Science and Engineering, Jilin University, Changchun, China, in 2015. He currently holds the post-doctoral position with the College of Chemistry, Jilin University.

His current research interests are in femtosecond laser induced periodic structures and its applications.

Xiao-Wen Cao received the B.S. degree from the School of Mechanical Science and Engineering, Jilin University, Jilin, China, in 2013. He is currently pursuing the Ph.D. degree with the School of Mechanical Science and Engineering, Jilin University.

His current research interests are in mechanism of femtosecond laser-matter interaction and femtosecond laser micro/nanomaching.

Chao Lv received the B.S. degree in electronic science and technology from the College of Physics, University of Science and Technology, Changchun, China, in 2012. She is currently pursuing the Ph.D. degree with the College of Electronic Science and Engineering, Jilin University.

Her current research interests are in design and laser fabrication of responsive hydrogel devices.

Hong Xia received the Ph.D. degree in polymer chemistry and physics from the College of Chemistry, Jilin University, Changchun, in 2006. He was a JST Postdoctoral Researcher with Osaka City University, Japan. From 2010 to 2011, he was Postdoctoral Researcher with the National Institute of Material Science, Tsukuba, Japan. In 2013, he was promoted as a Full Professor with the State Key Laboratory of Integrated Optoelectronics, Jilin University. His research interests include functional micronano-device fabrication and application based on femtosecond laser, optoelectronics of organic, and nanomaterials.

Wen-Jing Tian received the Ph.D. degree from the Changchun Institute of Applied Chemistry, Changchun, China, in 1993. She held associate professor position in 1996 and promoted as a Full Professor with the State Key Laboratory of Supramolecular Strucucture and Materials, Jilin University, in 2001. Her research interests are focus on design, synthesis, photon excitation mechanisms, photon emitting, and photovoltaic properties of opto-electrico supramolecular.

Qi-Dai Chen received the Ph.D. degree in plasma physics from the Institute of Physics, Chinese Academy of Sciences, Beijing, China, in 2004. He was a JST Postdoctoral Researcher with the Osaka City University of Japan. In 2006, he was employed as an Associate Professor with the College of Electronic Science and Engineering, Jilin University. In 2011, he was promoted as a Full Professor. His research interests include laser nanofabrication technology for micro-optics, semiconductor laser beam shaping, and subwavelength antireflective microstructure.

Saulius Juodkazis received the joint Ph.D. degree in experimental physics and material science from Vilnius University, Lithuania and Lyon-I University, France, in 1998. He held previous tenured positions with the Universities of Tokushima and Hokkaido in Japan. He is currently with the Centre for Micro-Photonics, Faculty of Science, Engineering and Technology, Swinburne University of Technology, and also with the Melbourne Centre for Nanofabrication in ANFF, Clayton, VIC, Australia. He has contributed to development of a 3-D femtosecond laser micro-fabrication for opto-fluidic, optical memory, and photonic crystal applications. His research is focused on the mechanisms and applications of light-matter interactions in small space and time domains, extreme pressure/temperature conditions. He is an OSA and SPIE Fellow.

Hong-Bo Sun received the B.S. and the Ph.D. degrees in electronics from Jilin University, Jilin, China, in 1992 and 1996, respectively.

He was a Postdoctoral Researcher with the Satellite Venture Business Laboratory, University of Tokushima, Japan, from 1996 to 2000, and then as an Assistant Professor with the Department of Applied Physics, Osaka University, Osaka, Japan. In 2005, he was promoted as a Full Professor (Changjiang Scholar), Jilin University, China. He has published over 200 scientific papers in the above field, which have been cited for over 9600 times according to ISI search report. His research has been focused on laser micro-nanofabrication in the past 10 years, particularly in exploring novel laser technologies including direct writing and holographic lithography, and their applications on micro-optics, micromachines, microfluids, and microsensors.